

# 1 **Assessing the perturbations of the hydrogeological regime in**

## 2 **sloping fens through roads**

3 Fabien Cochand<sup>1</sup>, Daniel Käser<sup>1</sup>, Philippe Grosvernier<sup>2</sup>, Daniel Hunkeler<sup>1</sup>, Philip Brunner<sup>1</sup>

4 <sup>1</sup>Centre of Hydrogeology and Geothermics, Université de Neuchâtel, Switzerland.

5 <sup>2</sup>LIN'eco, ecological engineering, PO Box 51, 2732 Reconvilier, Switzerland.

6

7 Corresponding author: Fabien Cochand, [fabien.cochand@unine.ch](mailto:fabien.cochand@unine.ch)

### 8 **Abstract**

9 Roads in sloping fens constitute a hydraulic barrier for surface and subsurface flow. This can lead to the  
10 drying out of downslope areas of the sloping fen as well as gully erosion. Different types of road construction have  
11 been proposed to limit the negative implications of the roads on flow dynamics. However, so far, no systematic  
12 analysis of their effectiveness has been carried out. This study presents an assessment of the hydrogeological  
13 impact of three types of road structures in semi-alpine, sloping fens in Switzerland. Our analysis is based on a  
14 combination of field measurements and fully integrated, physically-based modelling. In the field approach, the  
15 influence of the roads was examined through tracer tests where the upslope of the road was sprinkled with a saline  
16 solution. The spatial distribution of electrical conductivity downslope provided a qualitative assessment of the  
17 flow paths and thus the implications of the road structures on subsurface flow. A quantitative albeit not site-specific  
18 assessment was carried out using fully coupled numerical models jointly simulating surface and subsurface flow  
19 processes. The different road types were implemented and their influence on flow dynamics was assessed for a  
20 wide range of slopes and different hydraulic conductivities of the soil. The models are based on homogenous soil  
21 conditions, allowing for a relative ranking of the impact of the road types. For all cases analysed in the field and  
22 simulated using the numerical models, roads designed with an L-drain (i.e. collecting water upslope and releasing  
23 it in a concentrated manner downslope) constitute the largest perturbations in terms of flow dynamics. The other  
24 investigated road structures were found to have less impact. The developed methodologies and results can be used  
25 for the planning of future road projects in sloping fens.

## 26 1 Introduction

27 Wetlands can play a significant role in flood control (Baker, 2009;Zollner, 2003;Reckendorfer, 2013),  
28 mitigate climate change impacts (Cognard Plancq et al., 2004;Samaritani et al., 2011;Lindsay, 2010;Limpens,  
29 2008) and feature great biodiversity (Rydin, 2005). However, the world has lost 64% of its wetland areas since  
30 1900 and an even greater loss has been observed in Switzerland (Broggi, 1990). Therefore, wetland conservation  
31 has received considerable attention. However, the sprawl of human infrastructure, land-use changes, climate  
32 change or river regulations remain serious factors that threaten wetlands. For instance, roads can substantially  
33 modify the surface-subsurface flow patterns of sloping fens. The changes in flow patterns can influence sediment  
34 transport, moisture dynamics and biogeochemical processes as well as ecological dynamics.

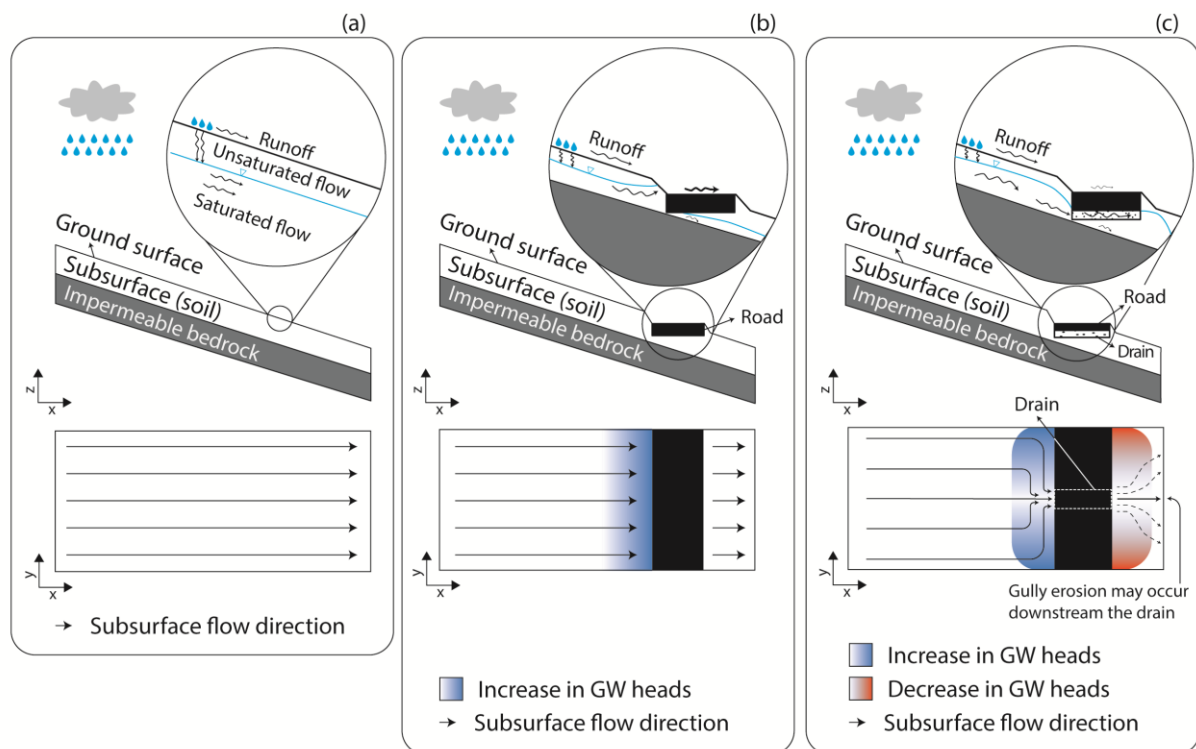
35 The link between hydrological changes and sediment dynamics has been studied in various contexts, see  
36 e.g. Partington et al. (2017). From a civil engineering perspective, erosion of the road must be avoided. A common  
37 strategy to avoid erosion of the road foundation is to collect water in drains and then release it in a concentrated  
38 manner downslope. This, however, can lead to erosion of the downslope area, a phenomenon known as « gully  
39 erosion ». A number of studies specifically focused on identifying the controlling processes and relevant  
40 parameters of gully erosion (Capra et al. 2009;Valentin et al. 2005;Descroix et al. 2008;Poesen et al.  
41 2003;Martínez-Casasnovas 2003;Daba et al. 2003;Betts and DeRose 1999;Derose et al. 1998). Nyssen et al. (2002)  
42 investigated the impact of road construction on gully erosion in the northern Ethiopian highlands, with a focus on  
43 surface water. In their study area, they observed the formation of a gully after the road construction downslope of  
44 the outlets of the drains. Based on fieldwork and subsequent statistical analysis, they concluded that the main  
45 causes for gully development are a concentrated runoff, the diversion of centered runoff to other catchments  
46 and the modifications of drainage areas induced by the road. The role of groundwater was not considered in this  
47 study.

48 Reid and Dunne (1984) developed an empirical model for estimating road sediment erosion of roads located  
49 in forested catchments in the Washington state (USA). They concluded that a heavily used road produced 130  
50 times more sediment than an abandoned road. Wemple and Jones (2003) also developed an empirical model for  
51 estimating runoff production of a forest road at a catchment scale. They demonstrated that during large storm  
52 events, subsurface flow can be intercepted by the road. The intercepted water, if directly routed to ditches, increases  
53 the rising limb of the catchment hydrograph. At a smaller spatial scale (0.1 km<sup>2</sup>), Loague and VanderKwaak (2002)  
54 assessed the impact of a road on the surface and subsurface flow using an integrated surface-subsurface flow model

55 InHM (Integrated Hydrology Model) (VanderKwaak, 1999) in a rural catchment. The results showed that the road  
56 induced a slight increase in runoff and a decrease of surface-subsurface water exchange around the road. Dutton  
57 et al. (2005) investigated the impact of roads on the near-surface subsurface flow using a variability saturated  
58 subsurface model. They concluded that the permeability contrast caused by the road construction leads to a  
59 disturbance of near-surface subsurface flow which may significantly modify the physical and ecological  
60 environment.

61 Road construction can also impact the development of vegetation (Chimner, 2016). Von Sengbusch (2015)  
62 investigated the changes in the growth of bog pines located in a mountain mire in the black forest (south-west  
63 Germany). The author suggests that the increase of bog pine cover is caused by a delayed effect of a road  
64 construction in 1983 along a margin of the bog. The road affects the subsurface flow and therefore prevents the  
65 upslope water to flow to the bog. According to von Sengbusch (2015), the road disturbances induce a larger  
66 variability in water table elevations during dry periods and consequently increase the sensitivity of the bog to  
67 climate change.

68 Based on these previous studies, a simple conceptual model describing the influence of roads in sloping  
69 fens on the flow system can be drawn (Figure 1). In natural conditions, rainwater infiltrates the soil and follows  
70 the topographical gradient. In case of heavy precipitation events, water can also directly flow on the surface (runoff  
71 in Figure 1a). To construct the foundation of the road, a material with very low permeability is used. This  
72 subsequently blocks the flow from the upslope towards the downslope. However, due to the buildup of hydraulic  
73 heads in the upslope of the road (Figure 1b), the road can be inundated during precipitation events. To reduce the  
74 occurrence of inundations, drains are installed under all roads (Figure 1c). The design and the materials of drains  
75 have potentially a significant effect on flow dynamics. Figure 1c presents a typical condition where a non-  
76 continuous drain (i.e., drains are perpendicularly installed at regular distances along the road) is installed. The  
77 drain captures the flow upslope along the road and the discharge is released in a concentrated manner downslope.  
78 This concentration of flow downslope may induce gully erosion and disturb the hydraulic regime of the sloping  
79 fens. For example, the wetland is at risk of drying out downslope of the road as the flow is concentrated to a small  
80 strip downslope of the drain. Note, however, that a gully must not necessarily develop because the flow-velocity  
81 at the drain-exit might not be sufficiently large to trigger erosion. Also, the drying out of the wetland beyond the  
82 direct vicinity of the downslope area of the drain must not necessarily happen. The concentrated release from the  
83 drain can, to a certain extent, spread out horizontally. In any case, a road constitutes a hydrogeological barrier that  
84 perturbs the natural flow dynamics.



85

86 **Figure 1: Conceptual subsurface dynamics in sloping fens: a) natural conditions, b) a road without a drain (only shown**  
 87 **for illustrative reasons as essentially all roads have drains). In this case, water will flow both across and under the road.**  
 88 **Uncontrolled flow beneath the road can cause erosion of the road foundation and c) a road with a drain, in this design,**  
 89 **surface water flow is reduced and flow beneath road occurs in a controlled manner through the drain. Water is released**  
 90 **downslope in a concentrated manner with the risk of gully erosion and the drying out of parts of the wetland. While it**  
 91 **is possible that the concentrated groundwater is redistributed horizontally downslope through natural heterogeneity,**  
 92 **there is a high risk of gully erosion.**

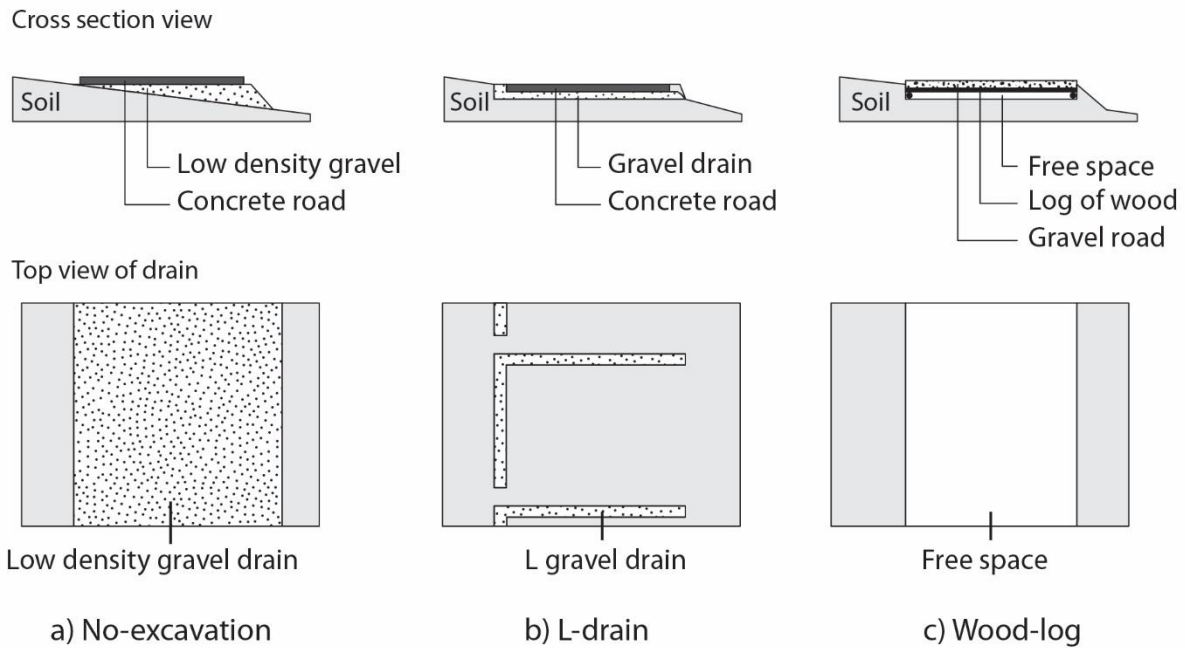
93 The design of the roads and especially the drains is expected to have a significant influence on the degree  
 94 of perturbation. Three fundamentally different road structures were developed in Switzerland to reduce the impacts  
 95 of roads. These three road types are conceptually illustrated in Figure 2. The efficiency of developed road structures  
 96 was so far not assessed after completion, neither in the field through field-based experiments, nor on a conceptual  
 97 level. This study focuses on these three road structures:

- 98 • The *no-excavation* structure (Figure 2a) aims at preserving soil continuity under the road. It consists of a  
 99 leveled layer of gravel, anchored to the ground, and underlying 0.16m thick concrete slabs. Soil  
 100 compaction is limited by using low-density gravel, made of expanded glass chunks (Misapor™) -  
 101 approximately fivefold lighter than conventional material.
- 102 • The *L-drain* structure (Figure 2b) aims at collecting subsurface water upslope the road and redirecting it  
 103 to discrete outlets on the other side. The setup consists of a trench, approximately 0.4m deep, filled with  
 104 a matrix of sandy gravel that contains an L-shaped band of coarse gravel acting as the drain. This is the  
 105 most common approach to build roads in Switzerland.

- 106       • The *wood-log* structure (Figure 2c) aims at promoting homogeneous flow under the road but does not  
107       preserve soil continuity. Embedded in a trench, approximately 0.4m deep, the wooden framework is filled  
108       with wooden logs forming a permeable medium. The wooden logs are then covered with mixed gravel.

109       In Switzerland, more than 20'000 ha are included in the national inventory of fens of national importance  
110 (Broggi 1990), most of them are located in the mountainous regions of the northern Prealps. These fens developed  
111 on nearly impermeable geomorphological layers such as silty moraine material or a particular rock layer named  
112 “flysch”. The majority of remaining Swiss fens are sloping fens in this particular geological environment. To  
113 protect the remaining wetlands, it is important to reduce the impact of these constructions, be it in the context of  
114 replacing existing, old roads or for the construction of new roads.

115       The aim of this study is to investigate the hydrogeological impact of the three road structures and their  
116 effects on fen water dynamics to support decision-makers in choosing road structures with minimal impact. A  
117 combination of fieldwork and hydrogeological modelling tasks was employed. Fieldwork was used to document  
118 the hydrogeological impact of existing road structures on fen water dynamics. It is the first time that these road-  
119 types are systematically analysed under field conditions. Sites with similar natural conditions were chosen to  
120 compare the influence of different road constructions on flow processes. The field studies allow for assessing the  
121 effectiveness of a given road structure at a particular location, however, they cannot provide a generalizable  
122 analysis of the different road types under different environmental and physical conditions. For example, critical  
123 environmental factors such as the slope or the bulk hydraulic properties of the fen will vary at different locations.  
124 This gap was filled by the development of generic numerical models. The most important hydraulic properties  
125 which control flow dynamics are explored systematically: the slopes of fens and the bulk hydraulic conductivity.  
126 The models are kept deliberately simple in terms of the heterogeneity of the soil. As the heterogeneity of the soil  
127 is not considered in the models, the horizontal redistribution due to field-specific heterogeneity cannot be  
128 considered (see figure 1c). The simulations thus constitute a “worst-case” scenario, which allows for a systematic  
129 comparison and a relative ranking of the different road structures in terms of perturbation and the risk for gully  
130 erosion.



131

132 **Figure 2 : Conceptual road structures, a) No-excavation road structure, b) L-drain road structure and c)**  
 133 **Wood-log road structure.**

134 **2 Methods**

135 **2.1 Study areas and fieldwork**

136 Four sloping fen areas located in alpine or peri-alpine regions of Switzerland (Table 1) were identified for  
 137 this study. All areas are situated in protected fen areas, and their selection was based on two main criteria:

- 138 1. The subsurface water flow must occur only in the topsoil layer and as runoff (as described in the  
 139 introduction).
- 140 2. The presence of roads constructed with either a no-excavation, L-drain and wood-log structure.

141 To fulfil the first criteria, soil profiles were analysed to ensure that each area with different road types had the  
 142 comparable soil stratigraphy: It had to be composed of organic soil on top of a layer of impermeable clay and  
 143 similar hydraulic regimes (e.g., runoff and subsurface flow occurring only in the topsoil layer). In addition, to  
 144 ensure that subsurface water is forced to cross the road instead of flowing in parallel of the road (and thus not  
 145 being affected directly by the road), another important criterion for the selection of the study areas was that  
 146 subsurface flow is perpendicular to the road.

147 To evaluate the hydraulic connection provided by the roadbed structures, tracer tests were carried out. As  
 148 illustrated schematically in Figure 3, the upslope area was irrigated with a saline solution and the occurrence of

149 the tracer was monitored downslope the road. In the absence of surface runoff, the occurrence of a tracer downslope  
 150 demonstrates the hydrogeological connection through the road. Furthermore, the spatial distribution of the tracer  
 151 front reflects the heterogeneity of the flow paths.

152 **Table 1. Field site locations and features.**

	<b>St-Antonien (STA)</b>	<b>Schoeniseischwand (SCH)</b>	<b>Stouffe (STO)</b>	<b>Höhmad (HMD)</b>
<i>Road type</i>	No excavation	L-Drain	Wood-log	Wood-log
<i>Terrain slope</i>	0.27	0.13	0.13	0.15
<i>WGS84 coordinates</i>	46.96760°N 9.84843°E	46.78872°N 7.96805°E	46.72957°N 7.83861°E	46.74027°N 7.89871°E

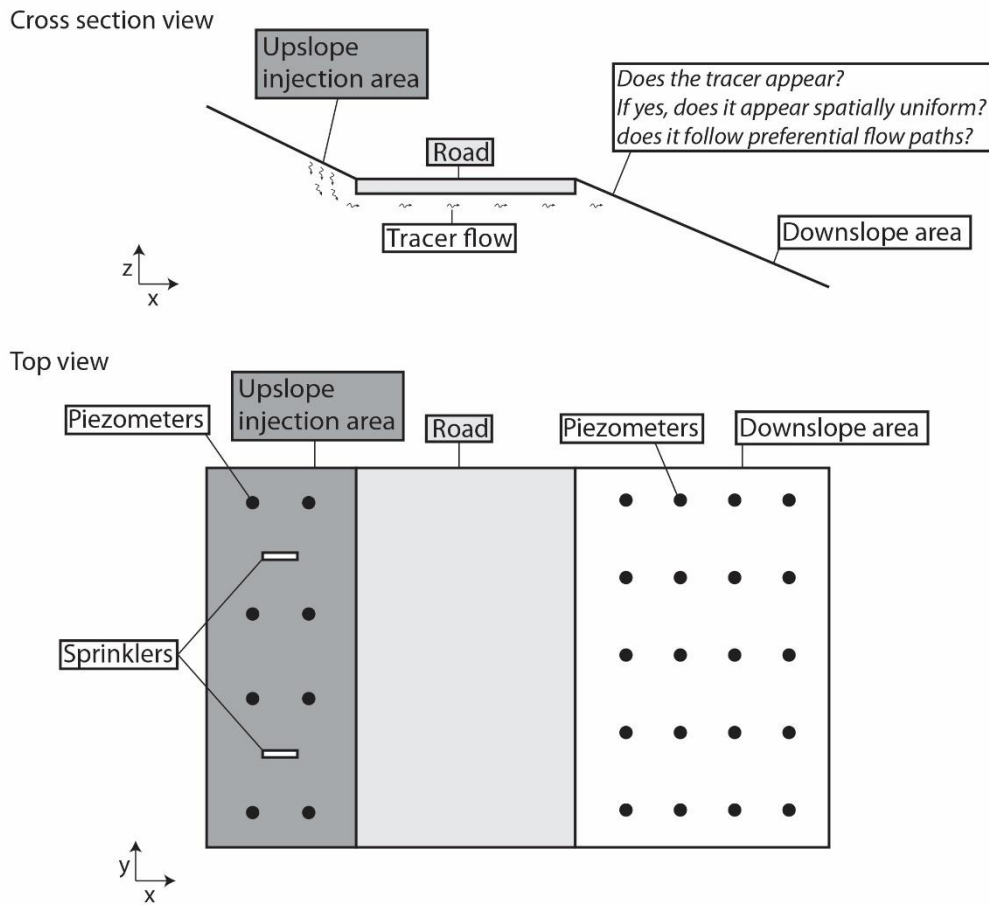
153

154 On each field site, an area of an 8 x 20m rectangle that includes a 2.5 to 3.5m wide road segment was  
 155 selected. A network of approximately 30 mini-piezometers on both sides of the road (Figure 3) was installed to  
 156 monitor the hydraulic heads and was used to obtain samples for the tracer test.

157 The mini-piezometers are high-density polyethylene (HDPE) tubes no longer than 1.5m (ID: 24mm). Each  
 158 tube was screened with 0.4mm slots from the bottom end to 5cm below ground level. It was inserted into the soil  
 159 after extracting a core with a manual auger (diameter: 4-6cm). The gap between the tube and the soil was filled  
 160 with fine gravel and sealed on the top with a 4cm thick layer of bentonite or local clay. Hydraulic heads were  
 161 measured using a manual water-level meter ( $\pm 0.3$ cm). At each point, the terrain and the top of the piezometer  
 162 were levelled using a level ( $\pm 0.3$ cm), whereas the horizontal position was measured with a tape measure ( $\pm 5$ cm).

163 The tracer tests were conducted using two oscillating sprinklers designed to reproduce a 30mm rain event  
 164 during 2-3 hours. This is equivalent to an intense rain event. Prior to the experiment, the sprinklers were activated  
 165 for 15-60 minutes to wet the soil surface. Sodium chloride was added to the irrigated solution to obtain an electrical  
 166 conductivity of 5-10mS/cm which is approximately ten times higher than the natural electrical conductivity of the  
 167 groundwater. Subsequently, the area (60m<sup>2</sup>) upslope of the road (upslope injection area of Figure 3) was irrigated  
 168 with the salt solution using the two sprinklers. The electrical conductivity (EC) of soil water was manually  
 169 measured using a conductivity meter in all mini-piezometers prior to the experiment, immediately after, and 24h  
 170 later. An increase in EC in piezometers located in the downslope area indicates that the injected saltwater flowed  
 171 from the upslope area to the downslope area below the road and clearly shows a hydraulic connection. Conversely,

172 if no changes in EC are observed in the piezometers, the hydraulic connection between up- and downslope of the  
173 road is affected.



174

175 **Figure 3 : Schematic view of the sites analysed during fieldwork.**

## 176 **2.2 Numerical modelling**

177 The modelling approach was structured in three steps. First, a 3D base case model representing surface and  
178 subsurface water flow in a sloping fen was elaborated. Subsequently, the base case model was modified to  
179 represent the three different types of road structures. For each model, various slopes, soil and road drain hydraulic  
180 conductivities were implemented to produce a sensitivity analysis and explore their sensitivities in the sloping fen  
181 flow dynamics (see section 2.2.3 for details).

### 182 **2.2.1 Numerical simulator**

183 The model used in the study is HydroGeoSphere (HGS) (Aquanty, 2017). HGS is a physically-based surface–  
184 subsurface fully-integrated model, based on the blueprint of Freeze and Harlan (1969), who proposed a model  
185 structure for jointly simulating surface- and subsurface flow-processes (Simmons et al., 2019). HGS is using the  
186 control volume finite element approach and solves a modified Richards' equation describing the 3D subsurface

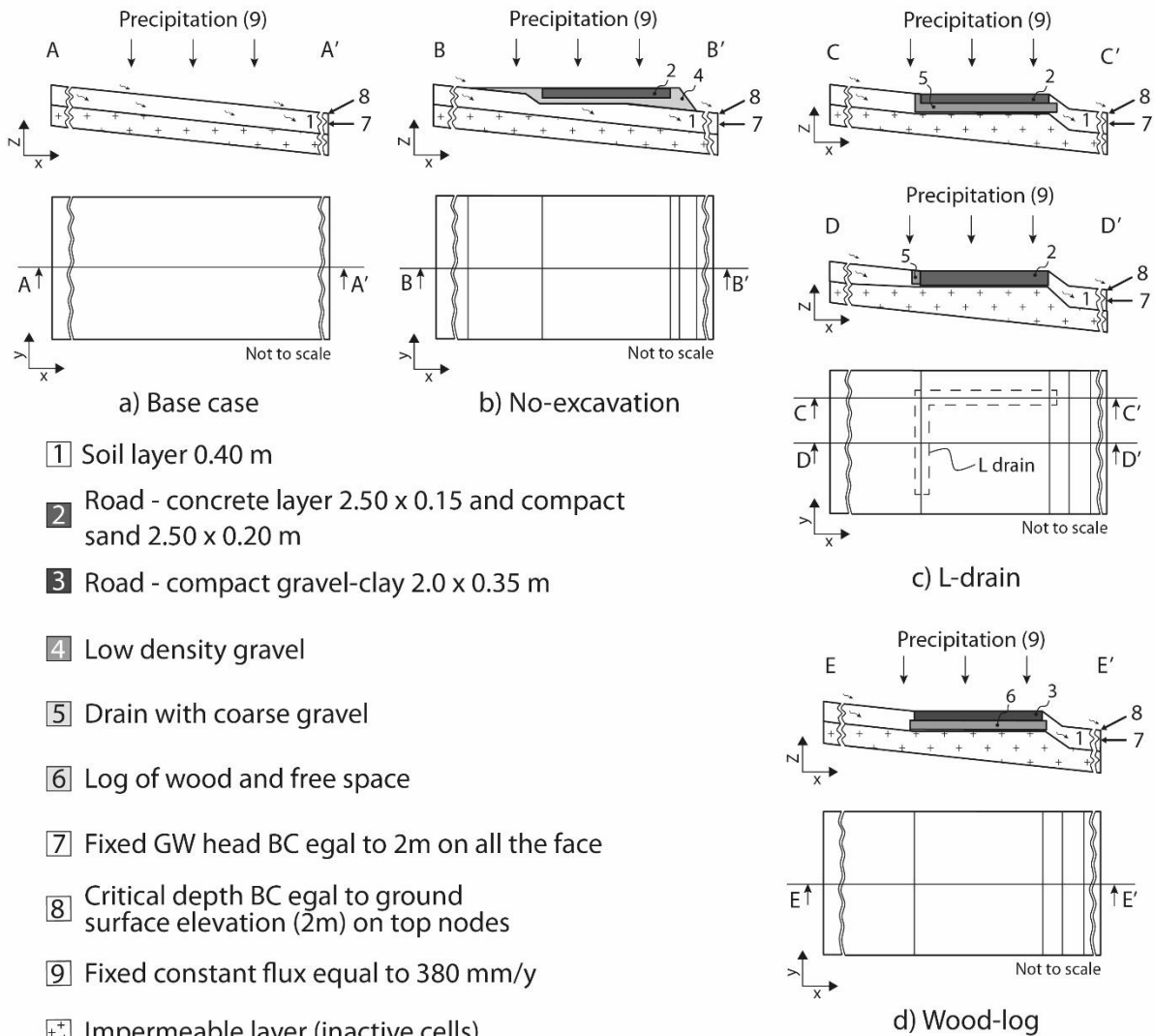


187 flow. If the subsurface flow is unsaturated, HGS employs the Van Genuchten (1980) functions to relate pressure  
188 head to saturation and relative hydraulic conductivity. Simultaneously, HGS solves the 2D depth-averaged  
189 diffusion-wave approximation of the Saint-Venant equation for describing the surface flow. To couple surface and  
190 subsurface and simulate the water exchanges between both domains, the “dual node approach” is used. In this  
191 approach, the top nodes representing the ground surface are used for calculating both subsurface and surface flow,  
192 the exchange flux between the two domains is calculated based on the head-difference between the surface and  
193 the subsurface and a coupling factor.

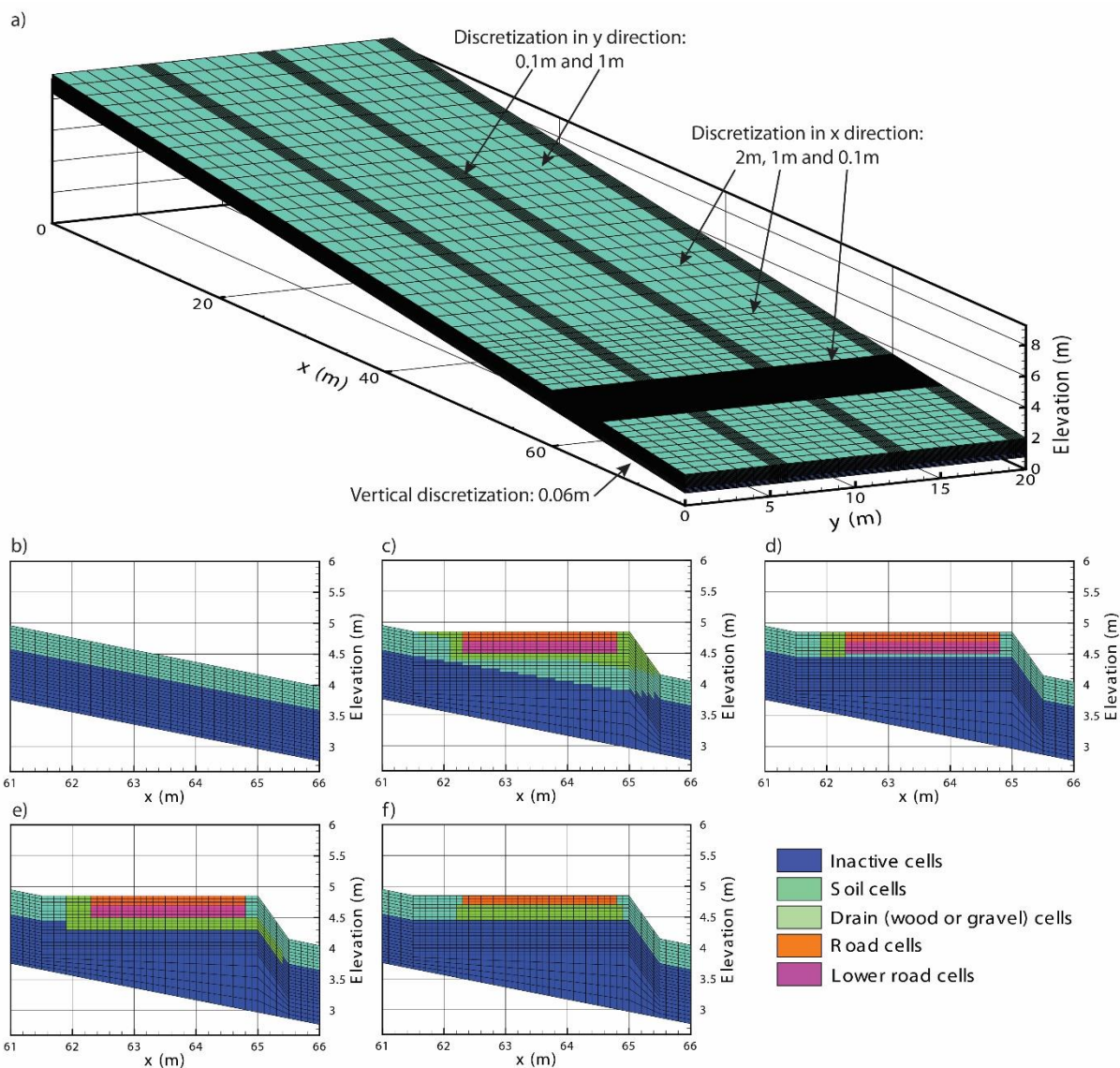
194 The iterative Newton-Raphson method is used to solve the nonlinear equations. At each subsurface node, saturation  
195 and groundwater heads are calculated, which allows for the calculation of the Darcy flux. For further details on  
196 the code, HGS capabilities and application, see Aquanty (2017), Brunner and Simmons (2012) or Cochand et al.  
197 (2019).

### 198 **2.2.2 Conceptual models and model implementation**

199 Figure 4 illustrates the conceptual model of each case. Existing engineering sketches were used as a basis  
200 for the implementation of the drain and road. Geometry, topography, and slopes are based on the conditions in the  
201 field. In each model, the soil layer has a thickness of 0.4m and the surface and subsurface water originated from  
202 precipitation only. The upslope boundary is the catchment boundary (water divide) and the downslope boundary  
203 represents the outlet of the model. Finally, it was assumed that the layer beneath the soil was impermeable (as  
204 observed in the field). One Neumann (constant flux) boundary condition was used on the top face for simulating  
205 precipitation. A constant head boundary condition (Dirichlet type) equal to the ground surface elevation (2m) was  
206 used on the lowest cells of the slope ( $x=76\text{m}$  on the Figure 5a) allowing groundwater to flow out of the model.  
207 Finally, a critical depth boundary condition which allows surface water to flow out of the model domain was  
208 implemented on the top nodes located at  $x=76\text{m}$ . All other faces are no-flow boundary conditions.



221 properties were adjusted. The fine spatial discretization of the mesh created between the coordinates  $61 < x < 66$   
 222 allows a more accurate representation of the simulated processes where high hydraulic gradients are expected (near  
 223 roads and drains).



224  
 225 **Figure 5 : Model development: a) Base case model, b) Base case model cross-section between  $61m < x < 66m$ , c) No-**  
 226 **excavation model between  $61m < x < 66m$ , d) L-drain model between  $61m < x < 66m$  along the transversal drain f) Wood-log model between  $61m < x < 66m$ .**  
 227

### 228 2.2.3 Model application

229 The model application consists of the variation of model properties to assess their effect on the groundwater  
 230 dynamics. The following parameters were analyzed: fen slope, soil hydraulic conductivities and road drain  
 231 hydraulic conductivities. These parameters were selected because according to Darcy's law (1) they control the  
 232 groundwater flow dynamics.  $K$  is the hydraulic conductivity of the soil and the drain and  $\nabla H$  the hydraulic gradient  
 233 of the fens which itself strongly influenced by the topographical slope.

$$q = K * \nabla H \quad (1)$$

234 For each property varied in the sensitivity analysis, three different values were chosen (Table 2): a low,  
 235 intermediate and high value. For the soil hydraulic conductivities (KS), values presented in Charman (2002) were  
 236 used and varied between 8.64m/d and 0.0864m/d. This corresponds to a soil composed of gravely organic matter  
 237 (as observed for example in St-Antonien site) or loamy organic matter (as observed for example in  
 238 Schoeniseischwand site). Van Genuchten parameters ( $\alpha$  and  $\beta$ ), as well as the residual water content, were not  
 239 varied. The road drains (KD) which are made of coarse or very coarse gravel were assigned a hydraulic  
 240 conductivity between 8640m/d and 86.4m/d (Fetter 2001), their van Genuchten parameters corresponding to  
 241 gravel. The slopes were fixed at 10%, 20% and 30%, as observed during fieldwork. The hydraulic conductivities  
 242 of the wood-log (W-L) drain were assumed ten times more conductive and more porous than the gravel drain. The  
 243 road concrete is almost impermeable and was thus conceptualized with a very low hydraulic conductivity, its van  
 244 Genuchten parameters corresponding to fine material. The road basement is constructed using highly compacted  
 245 fine material (sand and loam) and was thus implemented with low hydraulic conductivity, the van Genuchten  
 246 parameters corresponding to fine material. Finally, the implemented soil and road surface flow properties  
 247 correspond to a wetland and urban cover (Li et al., 2008).

248 *Table 2 : Subsurface and surface flow parameters.*

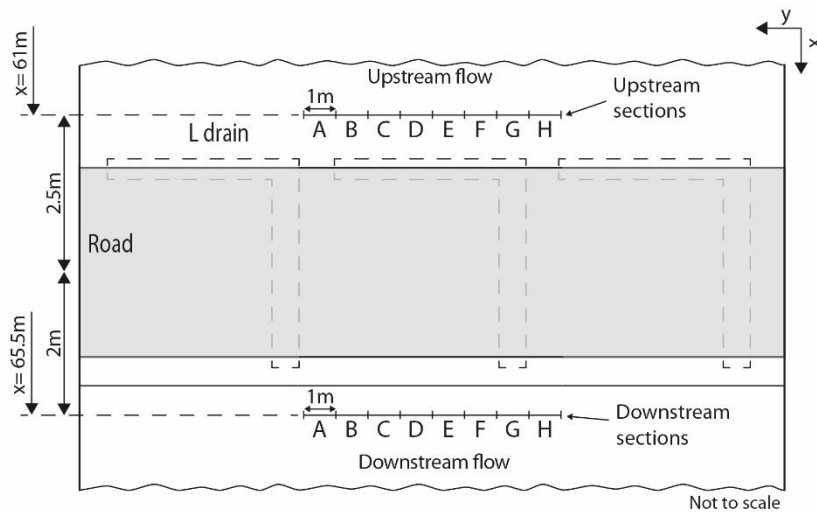
<b>Subsurface flow properties</b>					
	<b>Hydraulic conductivity</b>	<b>Porosity</b>	<b>Van Genuchten <math>\alpha</math></b>	<b>Van Genuchten <math>\beta</math></b>	<b>Residual water content</b>
<b>Units</b>	<b>K [md<sup>-1</sup>]</b>	<b><math>\theta</math> [-]</b>	<b><math>\alpha</math> [m<sup>-1</sup>]</b>	<b><math>\beta</math> [-]</b>	<b>Swr [-]</b>
<b>Soil - KS1</b>	8.64	0.25	4	1.41	0.04
<b>Soil - KS2</b>	0.864	0.25	4	1.41	0.04
<b>Soil - KS3</b>	0.0864	0.25	4	1.41	0.04
<b>Drains - KD1</b>	8640	0.25	29.4	3.281	0.04
<b>Drains - KD2</b>	864	0.25	29.4	3.281	0.04
<b>Drains - KD3</b>	86.4	0.25	29.4	3.281	0.04
<b>Drains - WL - KD1</b>	86400	0.7	29.4	3.281	0.04
<b>Drains - WL - KD2</b>	8640	0.7	29.4	3.281	0.04
<b>Drains - WL - KD3</b>	864	0.7	29.4	3.281	0.04
<b>Road concrete</b>	0.0000864	0.05	1.581	1.416	0.04
<b>Road basement</b>	0.00864	0.25	4	1.416	0.04

<b>Surface flow properties</b>					
	<b>Coupling length</b>	<b>Manning's roughness coefficient</b>		<b>Rill storage height</b>	<b>Obstruction height</b>
<b>Units</b>	<b><math>l_c</math> [m]</b>	<b><math>n_x</math> [m<sup>-1/3</sup>s]</b>	<b><math>n_y</math> [m<sup>-1/3</sup>s]</b>	<b><math>D_t</math> [m]</b>	<b><math>O_t</math> [m]</b>
<b>Soil</b>	$1. \times 10^{-2}$	0.03	0.03	0.005	0.005

Road	$1. \times 10^{-2}$	0.018	0.018	0.001	0.001
------	---------------------	-------	-------	-------	-------

249 In order to simulate each parameter combination, a total of 90 models were developed (27 models for each  
 250 road structure and 9 models for natural conditions). Models are run for 10'000 days (about 27 years) with a constant  
 251 flux equal to 380mm/y on the top representing the rainfall to reach a steady state. Subsequently, subsurface flow  
 252 rates in the soil layer were extracted at each section with an area of 0.4m<sup>2</sup> (1m wide times the soil thickness)  
 253 presented in Figure 6. Changes in subsurface flow rates indicate a perturbation of flow dynamics and therefore, a  
 254 comparison of flow rates between each model was made to present the effect of each road structure and sloping  
 255 fen properties on the dynamics.



256

257 **Figure 6 : Location of observation sections in the models.**

258 **3 Results and Discussion**

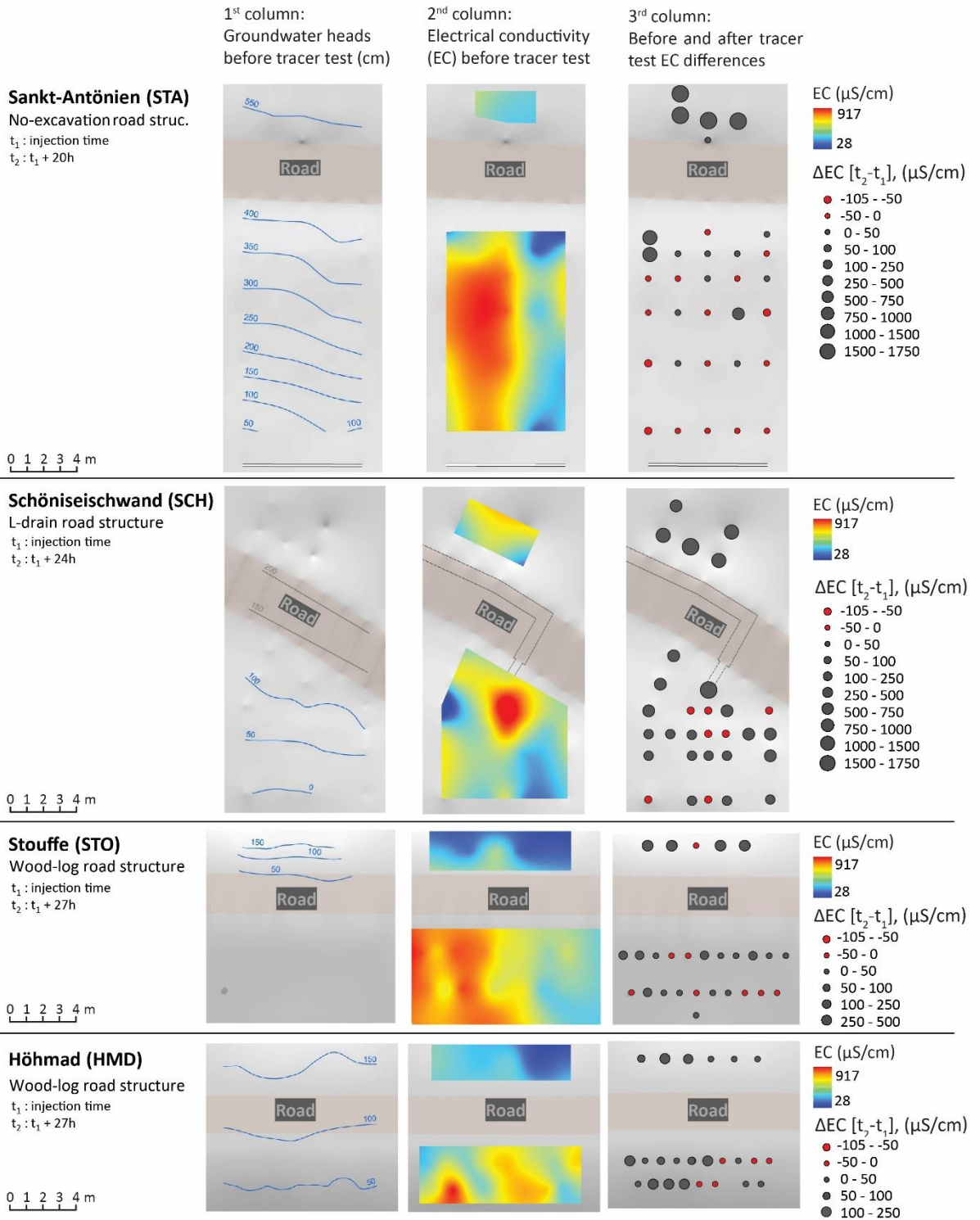
259 **3.1 Fieldwork**

260 Based on the observations, all sites show a continuous saturated zone before the experiment, both upslope and  
 261 downslope of the road, the hydraulic gradients being similar to the terrain slope (Figure 7, 1st column). In contrast,  
 262 the EC maps established prior to the tracer test show a spatial variability across one to several meters (Figure 7,  
 263 2nd column.). Within each plot, EC varies from 482 to 629μS/cm. At the SCH site, the highest values are located  
 264 downslope of the L-drain outlet which could indicate that the EC increases as water is flowing through the drain  
 265 (e.g. through the dissolution of the construction material). Given that this initial distribution of EC is not uniform,  
 266 the comparison of EC after the sprinkling experiment has to be made in a relative manner (Figure 7, 3rd column).

267 The heterogeneity of the hydraulic conductivity of the soil is apparent from the tracer tests (Figure 7, 3rd  
 268 column: EC 24 hours after injection). At all four sites, the front of the saline solution is not uniform because of the

269 heterogeneity of the soil hydraulic conductivity. Nevertheless, the road structures or the drains may create  
270 preferential flow paths. This is clearly occurring at the SCH site where the front follows two preferential flow  
271 paths. One related to the L-drain (right path) and the other on the left, unrelated to the L-drain, suggesting that the  
272 latter drains only a part of the water and the other part follows a natural preferential flow path. At the HMD site,  
273 the saline solution is far more concentrated on the left side of the plot, yet apparently not as a result of the road's  
274 structure. Rather, the soil appears more permeable on the left side of the plot, both upslope and downslope of the  
275 road. Finally, the decrease in EC observed 24 hours after injection at some locations might result from the  
276 following: (1) the tracer injection induces, by "piston effect", the displacement of a small volume of local water  
277 with a lower EC; (2) the tracer injection was preceded by a period of irrigation without tracer. This could have  
278 diluted the pre-irrigation soil solution.

279           In each case, the irrigation experiments demonstrate the continuity of subsurface flow under the road for  
280 all structures. For the no-excavation and wood-log type, the perturbation of the flow field seems to be controlled  
281 by the natural heterogeneity of the soil and flow paths, and not by the road itself. Conversely, the field data suggest  
282 that the L-drain constitutes a preferential pathway. This flow convergence can cause gully erosion.



283

284 **Figure 7 : Fieldwork results at the four field sites: 1<sup>st</sup> column) Measured groundwater heads before tracer test, 2<sup>nd</sup>**  
 285 **column) measured EC before tracer test and 3<sup>rd</sup> before and after tracer test differences in EC. The hydraulic heads**  
 286 **downslope the road in the Stouffe site is about 25cm and upslope the road in the Schöniseischwand is about 225cm**  
 287 **(between two isolines) and are not presented in the figure.**

288

## 289 3.2 Modelling

290 Figure 8a shows the results of the models with a slope of 10%, Figure 8b with a slope of 20% and Figure  
291 8b with a slope of 30%. In each dot chart, the groundwater flow rates (always in  $\text{m}^3/\text{d}$ ) are plotted with crosses for  
292 the base case model, diamonds for the no-excavation type, squares for the L-drain type and circles for the wood-  
293 log type. In addition, the maximum flow rate capacity of the soil calculated with Darcy's Law (1) and the flow  
294 rate induced by the precipitation are also presented for the interpretation of the results. In the following paragraphs,  
295 the base case (natural conditions) results are presented and discussed, followed by the simulations of the road  
296 structures.

297 In the base case model, groundwater flow rates vary from 0.003 ( $\text{m}^3/\text{d}$ ) to 0.069 ( $\text{m}^3/\text{d}$ ) for a 10% slope,  
298 0.006 ( $\text{m}^3/\text{d}$ ) to 0.069 ( $\text{m}^3/\text{d}$ ) for a 20% slope and from 0.009 ( $\text{m}^3/\text{d}$ ) to 0.069 ( $\text{m}^3/\text{d}$ ) for a 30% slope. The  
299 groundwater flow rate decreases following a decrease in the hydraulic conductivities (KS) of the soil layer. The  
300 groundwater flow rates are mainly controlled by the hydraulic conductivities, the slope plays a less important role.  
301 This is expected, as the ratios of the maximum and minimum hydraulic conductivity span two orders of magnitude,  
302 while slopes were multiplied by a factor of two (for a slope of 20%) or three (for a slope of 30%). Therefore,  
303 groundwater flow is increased by a factor 3 between the model KS3 with a slope of 10% and model KS3 with a  
304 slope of 30%. Concerning the formation of surface flow, the following observation can be made. For all KS2 and  
305 KS3 models, surface flow occurs while the infiltration capacity of the KS1 models is never exceeded and thus no  
306 surface flow occurs.

307 In the no-excavation and wood-log type models, the influence on flowrates caused by the presence of the  
308 road structures is quite similar. Groundwater flows vary from 0.01 ( $\text{m}^3/\text{d}$ ) to 0.069 ( $\text{m}^3/\text{d}$ ) for a 10% slope, 0.01  
309 ( $\text{m}^3/\text{d}$ ) to 0.069 ( $\text{m}^3/\text{d}$ ) for a 20% slope and to 0.010 ( $\text{m}^3/\text{d}$ ) to 0.069 ( $\text{m}^3/\text{d}$ ) for a 30% slope. Compared to the  
310 base case model, results show that the no-excavation and wood-log type structures have a minimal impact on flow  
311 perturbation. The only marked difference is that groundwater flow rates are slightly higher if the soil hydraulic  
312 conductivities are low (KS3). This is due to the hydraulic conductivity of the base of the road (consisting of wood-  
313 logs) higher than the hydraulic conductivity of the soil which facilitates infiltration. Conversely, in the base case  
314 model, less water is infiltrated but more surface runoff occurs. In the 20% and 30% slope models, the results of  
315 the no-excavation model are similar to the base case model.

316 In the L-drain model, the effect of the road is markedly different from the other road structures. The  
317 groundwater flows vary significantly in the observation sections. The maximum flows are always obtained in the

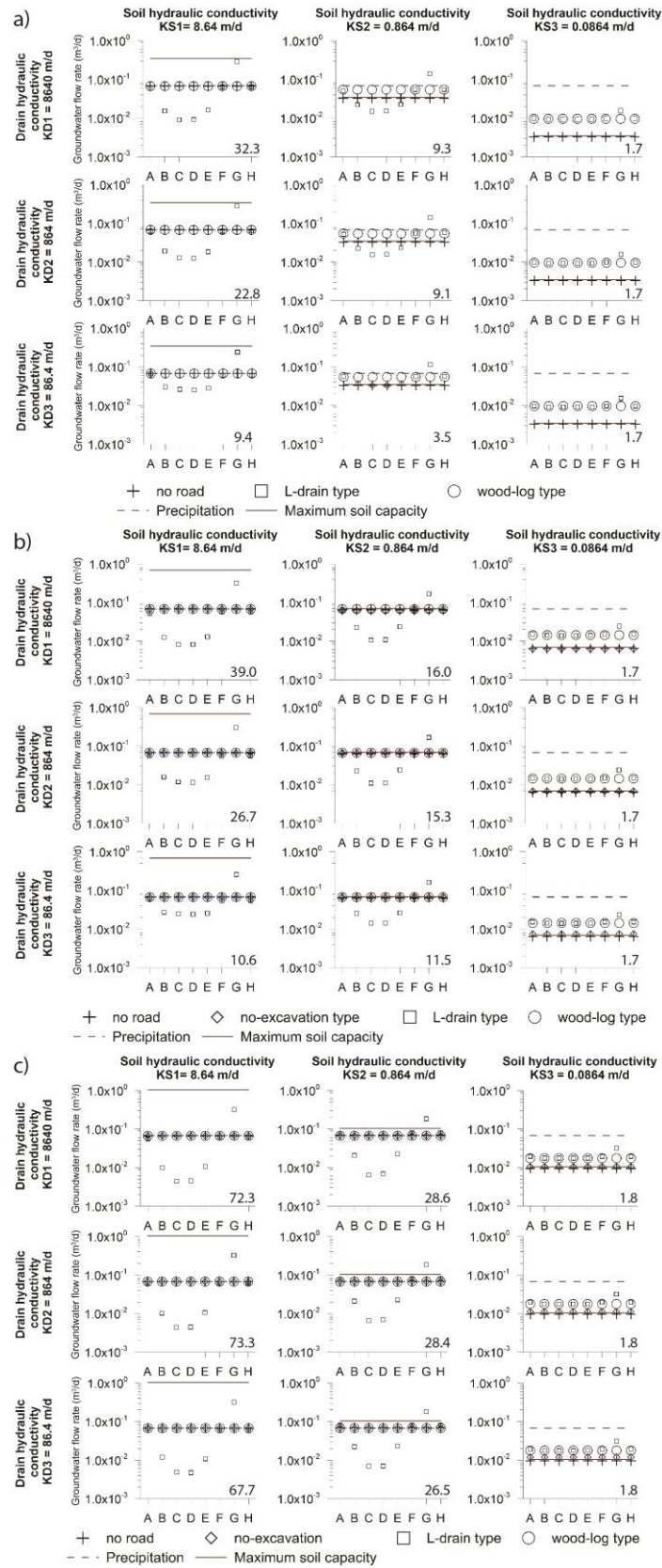


318 observation section G (see Figure 6 for the location of the sections) just downslope of the drain outlet and can be  
319 10 times higher than compared to the base case. Conversely, minimum flows are obtained in observation sections  
320 C and D in which flow rates can be 10 times lower. Significant differences in groundwater flow are also observed  
321 in the same transect (within the same model). To condense this information, the ratios between maximum and  
322 minimum flow rates are calculated for the L-drain structures (numbers at the bottom right of the panels in Figure  
323 8). The maximum differences are observed for the cases where the hydraulic conductivity of soil (KS) and drain  
324 (KD) are high and vary from 0.025 (m<sup>3</sup>/d) to 0.150 (m<sup>3</sup>/d). Conversely, when KS and/or KD is low, the differences  
325 along the transect are smaller. Finally, the slope accentuates groundwater flow rate differences along the transect.  
326 Therefore, an increase of groundwater flow differences is observed for the 10% and 30% slope scenarios, within  
327 the same model. The impact of the L-drain may be further explored by extracting groundwater flows lower than  
328 2m downslope the road to assess the extent of perturbations. Figure 9 shows simulated groundwater flows for the  
329 most critical cases (i.e. KS1 with a slope of 10%, 20% and 30%) downslope the road at 3.5m and 6.5m respectively  
330 and 2.5m upslope. At 3.5m groundwater flow regains the upslope conditions. At 6.5m downslope the road, all  
331 observation sections are very close to the upslope flows except in section G where flows are still slightly higher.

332 In addition to the assessment of perturbation through roads, the model results can be used to evaluate the  
333 risk of gully erosion. As presented in Figure 8, the maximum flow rate capacity of the soil is small in comparison  
334 to precipitation. For all model scenarios except for KS1, the soil capacity is lower than the precipitation and thus  
335 surface runoff occurs in the models and is likely to occur naturally. However, surface runoff may be triggered by  
336 the presence of L-drain structures. To illustrate this process, the simulated surface flow velocities of each road  
337 structure downslope the road for the model KS2-KD2 and slope of 20% are presented in Figure 10. In this case,  
338 the maximum flow rate capacity of the soil is approximately equal to precipitation, therefore runoff should not  
339 occur. However, this is not the case for the L-drain. The occurrence of surface runoff is the consequence of the  
340 subsurface flow concentration. In this configuration, the infiltration capacity of the soil is too small to  
341 accommodate the concentrated flow collected upslope, thus groundwater emerges and surface flow is triggered.  
342 This constitutes an increased risk of gully erosion. In addition, the perturbation of the roads upslope of the road  
343 was assessed.

344 Finally, the impact of road structure on the upslope road dynamics was also assessed (Figure not shown) 2.5m  
345 upslope. Upslope flows are similar to the base case model, thus the influence of the road is, not unexpectedly,  
346 marginal for all road types.

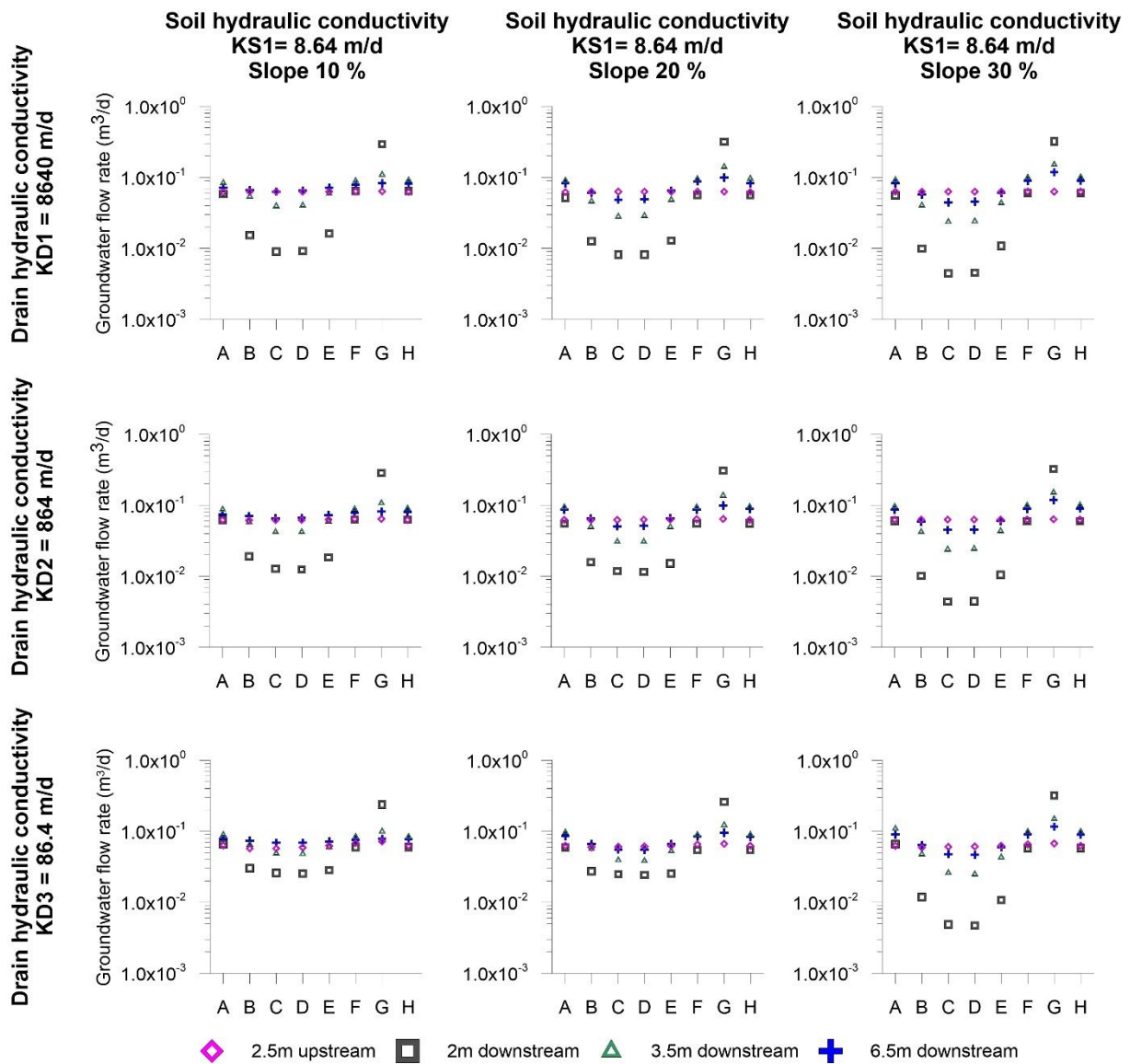
347           The development of models with various combinations of parameters allowed for exploring a larger  
348 parameter space than using fieldwork only. For instance, the fact that the impact of an L-drain structure on the  
349 water dynamics is less marked if the hydraulic conductivity of soil is low would have been impossible to identify  
350 by using fieldwork only. However, a numerical model is always a simplified reproduction of reality. The main  
351 model assumption is that the hydraulic conductivity of the soil is homogeneous- as opposed to the field conditions  
352 analyzed. However, the models are not intended to reproduce small-scale observations, i.e. the exact hydraulic  
353 head in a piezometer, but instead can be used to explore the influence of the road structures under different soil  
354 conditions (bulk hydraulic conductivities and slopes). Given that no heterogeneity-induced horizontal  
355 redistribution of the flow downslope can be simulated using homogeneous soil conditions, the models constitute  
356 a worst-case scenario. It is worst-case scenario because we exclude the possibility that through natural  
357 heterogeneity a fraction of the drained water could be horizontally redistributed downstream, thus potentially  
358 reducing the negative impact of the road. The models, therefore, allow for a relative ranking of the potential impact  
359 and clearly show the increased risk for surface water flow generation and thus gully erosion. For the investigated  
360 scenarios, the L-drain shows consistently the largest impact. The two other road structures are thus the preferred  
361 choice.



362

363  
364  
365

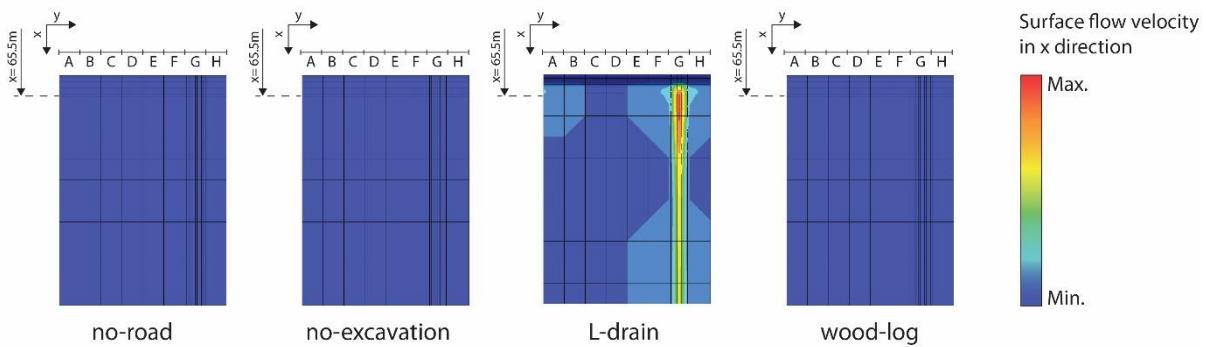
**Figure 8 : Simulated groundwater flow rates 2m downslope of each road structure and each parameter combination with a slope of a) 10%, b) 20% and c) 30%. Numbers at the bottom right of each panel are the ratio between maximum and minimum groundwater flow within the L-drain transect.**



367

368 **Figure 9 : Extent of perturbations due to the L-drain road type: Simulated groundwater flow rates different distances**  
 369 **the road.**

370



371

372 **Figure 10 : Simulated surface flow of the KS2-KD2 model and a slope of 20% for each road structure. The results**  
 373 **clearly indicate the increased risk caused by the L-drain of triggering surface runoff and thus potentially gully-**  
 374 **erosion and the drying out of sections of the wetland.**

375 **4 Conclusions**

376 This study assessed three road structures regarding their perturbations of the natural groundwater flow. Two  
 377 of these road structures were specifically developed to reduce the negative impacts of the road. The study is based  
 378 on two complementary approaches; field-based tracer tests and numerical models simulating groundwater flow for  
 379 the different road structures. The combination of fieldwork and the development of numerical models was  
 380 fundamental to achieve the goal of this study. The tracer test allowed for a better understanding of groundwater  
 381 flow throughout road structures and allowed for evaluating their effectiveness at a given location. However, the  
 382 tracer tests are time-consuming and only a few suitable field sites are available. Moreover, the results are site-  
 383 specific. The numerical approach, on the other hand, allows for exploring any combination of slope, hydraulic  
 384 properties or road structure, thus providing a more comprehensive approach aimed at a relative ranking of the  
 385 influence of the road structure. Given the simplified structure of the models, the results can not be directly used to  
 386 predict the influence at a specific field-site.

387 For all investigated scenarios, the significant impact of the L-drain road structure is clearly established and  
 388 is consistent with the field observations. For the other road structures too, the numerical models are consistent with  
 389 fieldwork results and show a relatively undisturbed groundwater flow downslope the road.

390 It is the first time that the performance of these road-structures has been investigated in the field. The tracer  
 391 tests showed that both sides of the road were hydraulically connected for all investigated road structures.  
 392 Groundwater flow was heterogeneous suggesting the occurrence of natural preferential flow paths in the soil. The  
 393 presence of a transversal drain (L-drain) beneath the road suggests that the L-drain constitutes a preferential flow  
 394 path of much greater importance than the naturally occurring preferential pathways. The field results further  
 395 suggest that the wood-log and no-excavation structures are less impactful than the L-drain. The simulation results

396 are consistent with the assessment of the relative impact of the different road-types. Groundwater flow rates 10  
397 times larger than in the natural case were obtained in the numerical simulations. The two other road structures  
398 (wood-log and no-excavation) do not perturb the flow field to the extent of the L-drain. To minimize the  
399 perturbation of flow fields, the wood-log and no-excavation structures are recommended.

## 400 **5 Acknowledgements**

401 This research was funded by the Swiss Federal Office for the Environment (FOEN) and supported by the  
402 Swiss Federal Office for Agriculture (FOAG). The authors are grateful to Benoit Magnin, Peter Staubli, Andreas  
403 Stalder, Anton Stübi and Ueli Salvisberger for their collaborations. We thank the three anonymous reviewers and  
404 the Editor, A: Hildebrandt, for her very detailed input to the paper.

## 405 **6 References**

- 406 Aquanty : HydroGeoSphere: A Three-Dimensional Numerical Model Describing Fully-Integrated  
407 Subsurface and Surface Flow and Solute Transport. Waterloo, ON, Canada: University of Waterloo,  
408 2017
- 409 Baker, C., Thompson, J. R. and Simpson, M.: 6. Hydrological Dynamics I: Surface Waters, Flood and  
410 Sediment Dynamics The Wetlands Handbook, 1st edition. Edited by E. Maltby and T. Barker. 2009.  
411 Blackwell Publishing, 120-168, 2009.
- 412 Betts, H. D., and DeRose, R. C.: Digital elevation models as a tool for monitoring and measuring gully  
413 erosion, International Journal of Applied Earth Observation and Geoinformation, 1, 91-101,  
414 [http://dx.doi.org/10.1016/S0303-2434\(99\)85002-8](http://dx.doi.org/10.1016/S0303-2434(99)85002-8), 1999.
- 415 Broggi, M. E.: Minimum requis de surfaces proches de l'état naturel dans le paysage rural, illustré par  
416 l'exemple du Plateau suisse. Liebefeld-Berne., Rapport 31a du Programme national de recherche "Sol",  
417 199p, 1990.
- 418 Brunner, P., and Simmons, C. T.: HydroGeoSphere: a fully integrated, physically based hydrological  
419 model, Groundwater, 50, 170-176, 2012.
- 420 Capra, A., Porto, P., and Scicolone, B.: Relationships between rainfall characteristics and ephemeral  
421 gully erosion in a cultivated catchment in Sicily (Italy), Soil and Tillage Research, 105, 77-87,  
422 <http://dx.doi.org/10.1016/j.still.2009.05.009>, 2009.
- 423 Charman, D.: Peatlands and environmental change. John Wiley & Sons Ltd. 301 2002.
- 424 Chimner, R. A., Cooper, D. J., Wurster, F. C. and Rochefort, L.: An overview of peatland restoration in  
425 North America: where are we after 25 years?, Restoration Ecology, 25, 283-292, 2016.
- 426 Cochand, F., Therrien, R., and Lemieux, J.-M.: Integrated Hydrological Modeling of Climate Change  
427 Impacts in a Snow-Influenced Catchment, Groundwater, 57, 3-20, doi:10.1111/gwat.12848, 2019.

428 Cognard Plancq, A. L., Bogner, C., Marc, V., Lavabre, J., Martin, C., and Didon Lescot, J. F.: Etude du rôle  
429 hydrologique d'une tourbière de montagne: modélisation comparée de couples "averse-crue" sur deux  
430 bassins versants du Mont-Lozère., *Etudes de géographie physique*, n° XXXI, p. 3 - 15, 2004.

431 Daba, S., Rieger, W., and Strauss, P.: Assessment of gully erosion in eastern Ethiopia using  
432 photogrammetric techniques, *CATENA*, 50, 273-291, [http://dx.doi.org/10.1016/S0341-](http://dx.doi.org/10.1016/S0341-8162(02)00135-2)  
433 [8162\(02\)00135-2](http://dx.doi.org/10.1016/S0341-8162(02)00135-2), 2003.

434 Derose, R. C., Gomez, B., Marden, M., and Trustrum, N. A.: Gully erosion in Mangatu Forest, New  
435 Zealand, estimated from digital elevation models, *Earth Surface Processes and Landforms*, 23, 1045-  
436 1053, [10.1002/\(SICI\)1096-9837\(199811\)23:11<1045::AID-ESP920>3.0.CO;2-T](https://doi.org/10.1002/(SICI)1096-9837(199811)23:11<1045::AID-ESP920>3.0.CO;2-T), 1998.

437 Descroix, L., González Barrios, J. L., Viramontes, D., Poulenard, J., Anaya, E., Esteves, M., and Estrada,  
438 J.: Gully and sheet erosion on subtropical mountain slopes: Their respective roles and the scale effect,  
439 *CATENA*, 72, 325-339, <http://dx.doi.org/10.1016/j.catena.2007.07.003>, 2008.

440 Dutton, A. L., Loague, K., and Wemple, B. C.: Simulated effect of a forest road on near-surface  
441 hydrologic response and slope stability, *Earth Surface Processes and Landforms*, 30, 325-338,  
442 [10.1002/esp.1144](https://doi.org/10.1002/esp.1144), 2005.

443 Freeze, R. A., and R, and Harlan, R.L.: Blueprint for a physically-based, digitally-simulated hydrologic  
444 response model, *Journal of Hydrology*, 9, 3, 237-258, [https://doi.org/10.1016/0022-1694\(69\)90020-1](https://doi.org/10.1016/0022-1694(69)90020-1),  
445 1969.

446 Li, Q., Unger, A. J. A., Sudicky, E. A., Kassenaar, D., Wexler, E. J., and Shikaze, S.: Simulating the multi-  
447 seasonal response of a large-scale watershed with a 3D physically-based hydrologic model, *Journal of*  
448 *Hydrology*, 357, 317-336, <http://dx.doi.org/10.1016/j.jhydrol.2008.05.024>, 2008.

449 Limpens, J., Berendse, F., Blodau, C., Canadell, J. G., Freeman, C., Holden, J., Roulet, N., Rydin, H. and  
450 Schaepman-Strub, G.: Peatlands and the carbon cycle: from local processes to global implications – a  
451 synthesis, *Biogeosciences*, 5, 1475-1491, 2008.

452 Lindsay, R.: Peatbogs and carbon: a critical synthesis to inform policy development in oceanic peat bog  
453 conservation and restoration in the context of climate change, University of East London, Technical  
454 Report, 2010.

455 Loague, K., and VanderKwaak, J. E.: Simulating hydrological response for the R-5 catchment:  
456 comparison of two models and the impact of the roads, *Hydrological Processes*, 16, 1015-1032,  
457 [10.1002/hyp.316](https://doi.org/10.1002/hyp.316), 2002.

458 Martínez-Casasnovas, J. A.: A spatial information technology approach for the mapping and  
459 quantification of gully erosion, *CATENA*, 50, 293-308, [http://dx.doi.org/10.1016/S0341-](http://dx.doi.org/10.1016/S0341-8162(02)00134-0)  
460 [8162\(02\)00134-0](http://dx.doi.org/10.1016/S0341-8162(02)00134-0), 2003.

461 Nyssen, J., Poesen, J., Moeyersons, J., Luyten, E., Veyret-Picot, M., Deckers, J., Haile, M., and Govers,  
462 G.: Impact of road building on gully erosion risk: a case study from the Northern Ethiopian Highlands,  
463 *Earth Surface Processes and Landforms*, 27, 1267-1283, [10.1002/esp.404](https://doi.org/10.1002/esp.404), 2002.

464 Partington, D., Therrien, R., Simmons, C. T., and Brunner, P.: Blueprint for a coupled model of  
465 sedimentology, hydrology, and hydrogeology in streambeds, *Reviews of Geophysics*, 55, 287-309,  
466 [10.1002/2016rg000530](https://doi.org/10.1002/2016rg000530), 2017.

467 Poesen, J., Nachtergaele, J., Verstraeten, G., and Valentin, C.: Gully erosion and environmental change:  
468 importance and research needs, *CATENA*, 50, 91-133, [http://dx.doi.org/10.1016/S0341-](http://dx.doi.org/10.1016/S0341-8162(02)00143-1)  
469 8162(02)00143-1, 2003.

470 Reckendorfer, W., Funk, A., Gschöpf, C., Hein, T. and Schiemer, F.: Aquatic ecosystem functions of an  
471 isolated floodplain and their implications for flood retention and management, *Journal of Applied*  
472 *Ecology*, 50, 119–128, 2013.

473 Reid, L. M., and Dunne, T.: Sediment production from forest road surfaces, *Water Resources Research*,  
474 20, 1753-1761, 10.1029/WR020i011p01753, 1984.

475 Rydin, H. a. J., J.: *The biology of peatlands*, Oxford University Press, 343p., 2005.

476 Samaritani, E., Siegenthaler, A., Yli-Petäys, M., Buttler, A., Christin, P.-A., and Mitchell, E. A. D.: Seasonal  
477 Net Ecosystem Carbon Exchange of a Regenerating Cutaway Bog: How Long Does it Take to Restore  
478 the C-Sequestration Function?, *Restoration Ecology*, 19, 480-489, 10.1111/j.1526-100X.2010.00662.x,  
479 2011.

480 Simmons, C.T., Brunner, P., Therrien, R., Sudicky, E.A.: Commemorating the 50th anniversary of the  
481 Freeze and Harlan (1969) Blueprint for a physically-based, digitally-simulated hydrologic response  
482 model. *J. Hydrol.* 124309. <https://doi.org/10.1016/J.JHYDROL.2019.124309>, 2019.

483 Valentin, C., Poesen, J., and Li, Y.: Gully erosion: Impacts, factors and control, *CATENA*, 63, 132-153,  
484 <http://dx.doi.org/10.1016/j.catena.2005.06.001>, 2005.

485 Van Genuchten, M. T.: A closed-form equation for predicting the hydraulic conductivity of unsaturated  
486 soils, *Soil science society of America journal*, 44, 892-898, 1980.

487 VanderKwaak, J. E.: Numerical simulation of flow and chemical transport in integrated surface-  
488 subsurface hydrologic systems, Ph.D. thesis, Departement of Earth Science, University of Waterloo,  
489 Waterloo, Ontario, Canada., 1999.

490 Von Sengbusch, P.: Enhanced sensitivity of a mountain bog to climate change as a delayed effect of  
491 road construction, *Mires and Peat*, 15: Art. 6, (Online: [http://www.mires-and-](http://www.mires-and-peat.net/pages/volumes/map15/map1506.php)  
492 [peat.net/pages/volumes/map15/map1506.php](http://www.mires-and-peat.net/pages/volumes/map15/map1506.php)), 2015.

493 Wemple, B. C., and Jones, J. A.: Runoff production on forest roads in a steep, mountain catchment,  
494 *Water Resources Research*, 39, 2003.

495 Zollner, A.: Das Abflussgeschehen von unterschiedlich genutzten Hochmooreinzugsgebieten - Bayer.  
496 Akad. f. Naturschutz u. Landschaftspflege - Laufen / Salzach, Laufener Seminarbeitr. , 111-119, 2003.